Oecologia (2010) 163:235–244
DOI 10.1007/s00442-009-1536-1

ECOSYSTEM ECOLOGY - ORIGINAL PAPER

Linking calcification by exotic snails to stream inorganic carbon cycling

Erin R. Hotchkiss · Robert O. Hall Jr.

Received: 27 June 2009 / Accepted: 1 December 2009 / Published online: 8 January 2010

Abstract Biotic calcification is rarely considered in freshwater C budgets, despite calculations suggesting that calcifying animals can alter inorganic C cycling. Most studies that have quantified biocalcification in aquatic ecosystems have not directly linked CO_2 fluxes from biocalcification with whole-ecosystem rates of inorganic C cycling. The freshwater snail, *Melanoides tuberculata*, has achieved a high abundance and 37.4 g biomass m^{-2} after invading Kelly Warm Springs in Grand Teton National Park. This high biomass suggests that introduced populations of *Melanoides* may alter ecosystem processes. We measured *Melanoides* growth rates and biomass to calculate the production of biomass, shell mass, and CO_2. We compared *Melanoides* biomass and inorganic C production with ecosystem C pools and fluxes, as well as with published rates of CO_2 production by other calcifying organisms. *Melanoides* calcification in Kelly Warm Springs produced 12.1 mmol CO_2 m^{-2} day^{-1} during summer months. We measured high rates of gross primary productivity and respiration in Kelly Warm Springs (−378 and 533 mmol CO_2 m^{-2} day^{-1}, respectively); CO_2 produced from biocalcification increased net CO_2 production in Kelly Warm Springs from 155 to 167 mmol CO_2 m^{-2} day^{-1}. This rate of CO_2 production via biocalcification is within the published range of calcification by animals. But these CO_2 fluxes are small when compared to ecosystem C fluxes from stream metabolism. The influence of animals is relative to ecosystem processes, and should always be compared with ecosystem fluxes to quantify the importance of a specific animal in its environment.

Keywords Biocalcification · Carbon cycling · Invasive species · *Melanoides tuberculata* · Stream metabolism

Communicated by Barbara Downes.

E. R. Hotchkiss (✉)
Program in Ecology, University of Wyoming,
Laramie, WY 82071-3166, USA
e-mail: ehotchki@uwyo.edu

E. R. Hotchkiss · R. O. Hall Jr.
Department of Zoology and Physiology,
University of Wyoming, Laramie, WY 82071-3166, USA

Introduction

CO_2 evasion from aquatic ecosystems is an important source of CO_2 that is not taken into account in many C budgets; most estimates of global C sources and sinks do not include freshwater ecosystems (Richey et al. 2002; Cole et al. 2007). Many freshwater ecosystems are supersaturated with CO_2 (Cole et al. 1994; Jones and Mulholland 1998), meaning that they are sources of CO_2 to the atmosphere. Aquatic CO_2 budgets assume that any changes in CO_2 concentrations are from gross primary productivity (GPP) and ecosystem respiration (ER), after accounting for groundwater inputs and exchange with the atmosphere (Wetzel 2001).

Most CO_2 budgets, especially in freshwater ecosystems, ignore biotic calcification (biocalcification) CO_2 fluxes from animals with $CaCO_3$ exoskeletons. When $CaCO_3$ exoskeletons are formed from dissolved Ca^{2+} and HCO_3^-, nearly 1 mol CO_2 is released for each mole of $CaCO_3$ fixed (Ware et al. 1991; Frankignoulle et al. 1994):

$$Ca^{2+} + 2HCO_3^- \leftrightarrow CaCO_3 + H_2O + CO_2. \quad (1)$$

Calcifying animals with high rates of secondary production can produce large fluxes of CO_2 in aquatic

ecosystems (Chauvaud et al. 2003; Golléty et al. 2008). CO_2 production through respiration or biocalcification may increase the amount of CO_2 released into the atmosphere. Increases in CO_2 production via biocalcification, linked with consumption of primary producers by consumers and allochthonous organic matter inputs, can raise local C emission budgets for invaded ecosystems (Schindler et al. 1997; Cole et al. 2000; Duarte and Prairie 2005).

Species-level influences on energy and nutrient cycling should be compared to whole-ecosystem fluxes in order to accurately understand the relative importance of biological processes in aquatic ecosystems. The few studies that have quantified CO_2 production from biocalcification in aquatic ecosystems have not compared calcification rates directly with CO_2 fluxes driven by GPP and ER. Comparing relative fluxes will be more biologically meaningful than reporting absolute values of CO_2 production via calcification. High biocalcification fluxes will require high rates of ecosystem metabolism, and the relative importance of calcification may be small when compared to whole-ecosystem inorganic C fluxes.

Here we evaluate the calcification-driven CO_2 fluxes of an exotic snail population relative to ecosystem-level CO_2 fluxes. *Melanoides tuberculata* have established a population with high abundance and biomass in Kelly Warm Springs, Grand Teton National Park, suggesting *Melanoides* have the potential to change the elemental cycling and productivity of invaded habitats, as have mollusks in other ecosystems (Strayer et al. 1999; Chauvaud et al. 2003; Hall et al. 2003). To estimate the impacts of *Melanoides* on C cycling in Kelly Warm Springs, we asked:

1. How much CO_2 is released into stream water through $CaCO_3$ shell synthesis by *Melanoides*?
2. To what degree do snails alter inorganic C cycling relative to GPP and ER?

To answer these questions, we measured growth rates, biomass, and shell mass of *Melanoides* in Kelly Warm Springs to calculate rates of organic and inorganic C production, and translated shell growth rates into rates of CO_2 production via calcification. We also compared these snail-driven rates with estimates of GPP, ER, concentrations of carbonate species, and net CO_2 flux into the atmosphere.

Materials and methods

Study site and *Melanoides* life history

Kelly Warm Springs is in Grand Teton National Park (Wyoming, USA; 43°38′21.8″N, 110°37′01.9″W). The average width and depth of Kelly Warm Springs are 3.9 and 0.12 m, respectively. Stream velocity and discharge are relatively constant at 15.5 m min^{-1} (SD = 1.3) and 7.47 m^3 min^{-1} (SD = 0.05). The fish assemblage in Kelly Warm Springs includes many non-indigenous species, with established populations of swordtail (*Xiphophorus helleri*), tiger barb (*Puntius tetrazona*), convict cichlid (*Cichlasoma nigrofasciatum*), guppy (*Poecilia reticulata*) and tilapia (*Tilapia* sp.), presumably from aquarium-dumping (United States Geological Survey 2005). In summer 2003, we observed *Melanoides* in Kelly Warm Springs, and while we do not know the exact date of introduction, *Melanoides* were absent from invertebrate samples collected in 2001 (R. O. Hall and E. R. Hotchkiss, unpublished data).

Melanoides tuberculata (Gastropoda, Thiaridae) are likely native to eastern Asia but have established populations throughout the globe (Robinson 1999; Facon et al. 2003). Invasive populations of *Melanoides* are closely linked with the aquarium trade, and are limited to warm fresh and brackish waters with temperatures ranging from 14 to 31°C (Dudgeon 1986; Duggan 2002). Individuals can grow up to 35 mm in length, which is likely equivalent to 3–5 years in age (Dudgeon 1986; Duggan 2002; Rader et al. 2003). *Melanoides* are parthenogenetic and viviparous; embryos develop in the mother and young range from 1.0 to 4.0 mm in length when they are released from the brood pouch (Berry and Kadri 1974; Subba Rao and Mitra 1982).

Melanoides production

During June–September 2006, we sampled all benthic macroinvertebrates along a 504-m reach of Kelly Warm Springs. We collected monthly samples from six sites along the reach using a 15.2-cm diameter stovepipe sampler (Hall et al. 2006). We sorted, counted and measured macroinvertebrates using 1-mm and 250-μm sieves to separate size fractions. We used digital calipers to measure *Melanoides* shell lengths to the nearest 0.1 mm. Each 250-μm to 1-mm fraction of benthic samples was sub-sampled following Hall et al. (2006). All macroinvertebrates were preserved in 95% ethanol.

We developed length/mass regressions for biomass and shell mass using unpreserved *Melanoides*. We dried, weighed, ashed (at 500°C for 4 h) and re-weighed 27 different size groups of *Melanoides* that included a total of 157 individuals, ranging from 1.9 to 21.2 mm in length, grouped in 0.5-mm increments. Biomass was the difference between dry and ashed mass [mg ash-free dry mass (AFDM)]. The relationship between shell length and biomass was: [biomass (mg AFDM)] = 0.0021[shell length (mm)]$^{3.12}$ ($n = 27$, $r^2 = 0.96$, $P < 0.0001$). Shell mass (mg $CaCO_3$) was calculated from ashed weights. The relationship between shell length and shell mass was: [shell mass (mg $CaCO_3$)] = 0.0223[shell length (mm)]$^{2.97}$

($n = 27$, $r^2 = 0.99$, $P < 0.0001$). This method does include body ash in the total $CaCO_3$ calculations for *Melanoides*; pleurocerid snails (*Elimia*) have an average body ash percent of 19% (Benke et al. 1999) and *Melanoides* biomass is less than 15% of their combined shell mass and biomass. Including body ash in shell ash calculations resulted in ~3% error by using total ash for shell ash estimates.

We calculated size-specific biomass and shell mass for *Melanoides* using the equations relating shell length to biomass and shell mass. To estimate confidence intervals (CIs) for biomass and shell mass samples, we used a bootstrap analysis (R Development Core Team 2009) to sample 1,000 times with replacement for mean biomass and shell mass densities for each of the 4 months we sampled *Melanoides* populations. We calculated the monthly mean of the four bootstrap vectors, and used the grand mean (the 50% percentile) and 90% CIs (between the 5 and 95% quantiles) of bootstrap estimates across all sampling dates to calculate *Melanoides* biomass (mg AFDM m^{-2}) and shell mass (mg $CaCO_3$ m^{-2}).

To estimate shell and biomass specific growth rates, we measured in situ growth rates of *Melanoides* ranging from 1.5 to 13 mm in length during July and August 2006. Size classes were binned in 0.5-mm shell length increments. We placed four to eight individuals from one size class with a small rock and attached algae (free of macroinvertebrates) in 56 × 43-mm tea infuser growth cages with 244-μm nylon mesh (Toby TeaBoy; Hall et al. 2006). *Melanoides* densities in growth cages corresponded to the lower end of ambient densities (to avoid food limitation in cages at the end of the incubation) at ~5,000 individuals m^{-2}. Growth cages were incubated for 21 days in Kelly Warm Springs. We preserved individuals from each growth cage at the end of the 3-week incubation. We re-measured shell lengths to calculate biomass and shell mass, from which we estimated specific growth rates for snails in each growth cage:

$$\text{Specific growth rate } (\text{day}^{-1}) = \frac{\ln \text{mass}_t - \ln \text{mass}_0}{t} \quad (2)$$

where $mass_0$ is the initial mass of the individuals in the growth cage, $mass_t$ is the mass of the individuals at the end of the growth period, and t is the incubation length (day). Because growth rates depend on ranges in temperature, we recorded temperatures throughout the entire incubation, using dataloggers (HOBO Water Temp Pro v2; Onset Computer Corporation) secured to the bottom of the 0- and 504-m sites. We regressed size-specific growth with shell length using SAS PROC REG (SAS Institute 2002–2003) to find the best predictive regression for the relationship between shell length and growth rate for all size classes.

After measuring size-specific growth rates and biomass for *Melanoides* in Kelly Warm Springs, we calculated instantaneous secondary biomass production (P_M; mg AFDM m^{-2} day^{-1}) and shell production (P_S; mg $CaCO_3$ m^{-2} day^{-1}) for each sampling month:

$$\text{Somatic secondary production} = \sum_{i=1}^{n} g_i B_i \quad (3)$$

where g_i is size-weighted specific growth rate (day^{-1}) and B_i is size-weighted biomass (mg AFDM m^{-2}) or shell mass (mg $CaCO_3$ m^{-2}) for the ith size class of snails (Benke 1984). These biomass and shell mass monthly production rates (P_M and P_S) were used to calculate the ratio of biomass P_M to monthly biomass (P:B) as well as the ratio of shell mass P_S to monthly shell mass estimates for *Melanoides*. To account for uncertainty in biomass and shell mass measurements, we used these monthly ratios from our collected data and the bootstrap mean biomass or shell mass for each sampling month to calculate the mean rates of *Melanoides* biomass production (mg AFDM m^{-2} day^{-1}) and shell mass production (mg $CaCO_3$ m^{-2} day^{-1}) in Kelly Warm Springs:

$$\text{Bootstrap secondary production} = b_x \left[\frac{P_x}{B_x}\right] \quad (4)$$

where b_x is the mean bootstrap estimate for biomass (b_M; mg AFDM m^{-2}) or shell mass (b_S; mg $CaCO_3$ m^{-2}) for each month, and $\left[\frac{P_x}{B_x}\right]$ is the ratio of production (P_M or P_S) to biomass (B_M) or shell mass (B_S) for each month (day^{-1}) calculated using the monthly size-weighted production and mass from stovepipe samples. We averaged these rates of bootstrap secondary production over all 4 months for the final values used to calculate $CaCO_3$, CO_2, and biomass production.

Because somatic growth data did not include fecundity, we also estimated fecundity for *Melanoides* to compare the relative contribution of reproduction (vs. growth) to total biomass production. Fecundity calculations were based on the observation that juvenile snails were approximately 1.5 mm long at the time of emergence from the brood pouch. We measured the dry mass and AFDM of the smallest *Melanoides* collected from Kelly Warm Springs for calculations of biomass and shell mass production. We chose a conservative reproduction rate of 182 juveniles $year^{-1}$ $individual^{-1}$ for all fecund individuals between 12.0 and 25.0 mm in length (Berry and Kadri 1974; Subba Rao and Mitra 1982); assuming reproduction occurs continuously throughout the year for scaled-up annual P:B comparisons (Dudgeon 1986; Pointier et al. 1992).

C cycling

We measured GPP and ER (g O_2 m^{-2} day^{-1}) using a two-station, open-channel, dissolved oxygen method (Odum

1956). We placed two Hydrolab MiniSondes (Hach Environmental) in Kelly Warm Springs at either end of a 504-m reach during July and August 2006 to measure changes in dissolved O_2 concentrations every 10 min for 2- to 3-day cycles. Using measurements of width, depth, travel time, and k_{O_2}, we calculated instant metabolism throughout seven different 24-h cycles (Hall et al. 2007):

$$\text{Instant metabolism}\left(\text{g O}_2\ \text{m}^{-2}\ \text{min}^{-1}\right) = z\left[\frac{(C_t - C_0)}{j}\right] - k_{O_2}(\text{DO}_{\text{Def}}) \quad (5)$$

where C_t and C_0 are the dissolved oxygen concentrations at downstream and upstream sites (g O_2 m^{-3}), j is water travel time between the 0- and 504-m reach (min), k_{O_2} is the piston velocity for O_2 (m min^{-1}, calculations via SF_6 tracer addition explained below), DO_{Def} is the average of the dissolved oxygen deficit relative to saturation (i.e., $O_{2sat} - O_2$) measured upstream and downstream (g O_2 m^{-3}), and z is stream depth (m). We found no groundwater inputs along the 504-m reach using NaCl tracer additions; therefore, we did not correct metabolism estimates for groundwater (Hall and Tank 2005). We calculated ER assuming that ER during the daytime was equal to ER at night; GPP was calculated as the area under each diel O_2 curve (Odum 1956; Hall et al. 2007). We converted O_2 metabolism calculations to CO_2 using a photosynthetic quotient of 1.2 (Raine 1983) and a respiratory quotient of 1.0 (Williams and del Giorgio 2005).

We used a one-station, open-channel metabolism method during two periods in July because only one MiniSonde was operating at that time. After comparing GPP and ER calculated using the two-station and the one-station approaches for the dates when we deployed two MiniSondes (details in "Results"), we included our one-station calculations from the end of July in our overall estimates of metabolism for Kelly Warm Springs.

To measure air–water gas exchange with respect to O_2 and CO_2 fluxes, we used tracer additions of SF_6. SF_6 evades at a rate proportional to that for O_2 and CO_2 (Wanninkhof et al. 1990; Cole and Caraco 1998). We also added a conservative tracer, NaCl, to calculate water travel time and dilution from groundwater inputs along the reach (Wanninkhof et al. 1990). We collected triplicate dissolved gas samples at five stations along an 800-m reach downstream from the release site, and measured the decline in SF_6 concentrations using a gas chromatograph with an electron capture detector (Shimadzu gas chromatograph 14A). Piston velocity (k_{SF_6}; m min^{-1}), was calculated from three separate SF_6 releases using stream depth, velocity and the gas transfer coefficient (K_{SF_6}; m^{-1}), measured from the decline in SF_6 downstream. We used our average k_{SF_6} to calculate k_{600}, k_{O_2} and k_{CO_2} from the ratios of gas transfer velocities and temperature-adjusted Schmidt numbers for the gas of interest, where k_{600} is calculated using a Schmidt number of 600 (Wanninkhof 1992; Cole and Caraco 1998).

We measured several water chemistry and physical parameters during four diel sampling events and during the day on a weekly basis throughout summer 2006 at upstream (0 m) and downstream (504 m) sites along our reach. These data included temperature, acid-neutralizing capacity (ANC) calculated by titration (Wetzel and Likens 2000), pH (Orion 3-star portable pH meter with a ROSS Ultra® pH electrode; Thermo Scientific), conductivity and dissolved O_2 (Hydrolab MiniSondes; Hach Environmental). We collected duplicate 60-ml water samples from upstream and downstream sites; we filtered, froze, and later analyzed them for concentrations of common cations and anions (Dionex ICS-2000 ion chromatography system with AS40 automated sampler and Perkin Elmer 372 atomic absorption spectrophotometer). We also measured stream width (w; m) and velocity (v; m min^{-1}) several times during summer 2006 using a flow meter (Marsh-McBirney) and meter tape. Stream discharge (Q; m^3 min^{-1}) was calculated using velocity and depth measurements from multiple transects along the 504-m reach. Effective stream depth (z; m) was $z = \frac{Q}{w \cdot v}$.

Using pH, temperature and ANC, we calculated dissociation constants for carbonic acid, carbonate species concentrations, and total dissolved inorganic C. Carbonic acid dissociation constants (K_1 and K_2) were calculated using adjustments for temperature (Cai and Wang 1998). We calculated the concentrations of different carbonate species using measurements of ANC, pH, and carbonic acid dissociation constants, following Millero (1979):

$$\left[H_2CO_3^*\right] = H_2CO_3 + CO_2 = \frac{\left(\frac{A_C a_H}{K_1}\right)}{\left(1 + \frac{2K_2}{a_H}\right)} \quad (6)$$

$$\left[HCO_3^-\right] = \frac{A_C}{1 + \frac{2K_2}{a_H}} \quad (7)$$

$$\left[CO_3^{2-}\right] = \frac{A_C K_2}{a_H + 2K_2} \quad (8)$$

where brackets represent the effective concentration in mmol m^{-3}, A_C is ANC (mmol m^{-3}) and a_H is the activity, or effective concentration of H^+. Total dissolved inorganic C is the sum of $[H_2CO_3^*]$, $[HCO_3^-]$ and $[CO_3^{2-}]$. We calculated partial pressure of CO_2 (atm) using indirect measurements of $[H_2CO_3^*]$ and Henry's constant for CO_2 (K_H; mmol m^{-3} atm^{-1}) corrected for temperature and elevation (Langmuir 1997):

$$pCO_2 = \frac{\left[H_2CO_3^*\right]}{K_H}. \quad (9)$$

We calculated CO_2 fluxes from Kelly Warm Springs by multiplying the CO_2 deficit by the site-specific piston velocity for CO_2:

$$\text{Instant metabolism}\left(\text{g O}_2\ \text{m}^{-2}\ \text{min}^{-1}\right) = z\left[\frac{(C_t - C_0)}{j}\right] - k_{\text{O}_2}(\text{DO}_{\text{Def}}) \quad (10)$$

where k_{CO_2} is the piston velocity for CO_2 (m min^{-1}), pCO_2 is the partial pressure of CO_2 (atm), K_H is the Henry's constant for CO_2 (mmol m^{-3} atm^{-1}), and $[CO_2]_{sat}$ is the concentration of CO_2 (mmol CO_2 m^{-3}) at saturation (Cole and Caraco 1998). A positive CO_2 flux value represents CO_2 flux out of the stream and into the atmosphere.

Contributions of *Melanoides* to C cycling

We measured the rate of CO_2 flux into the atmosphere and the extent to which *Melanoides* were responsible for making Kelly Warm Springs a source of CO_2. Using growth rates in combination with the $CaCO_3$ content of varying shell sizes, we calculated the mass of $CaCO_3$ produced by *Melanoides* (see secondary production calculations) and, consequently, the CO_2 emitted through shell synthesis during summer months. We calculated the ratio of released CO_2 to fixed $CaCO_3$ (Ψ) using temperature and salinity adjustments (Frankignoulle et al. 1994).

Results

Melanoides production

Melanoides persisted at high densities 1.5 km downstream of the spring pool and at low densities along 0.5 km of a lower reach before Kelly Warm Springs merged with Ditch Creek, a tributary to the Snake River (E. R. Hotchkiss, personal observation). The density of *Melanoides* in the 504-m reach averaged 29,600 individuals m^{-2} (SD = 20,500) in summer 2006. The mean biomass of *Melanoides* was 37.4 g AFDM m^{-2} (90% bootstrap CI = 29.9–45.2). Biomass of native mollusks, arthropods, and annelids was 4.9 g AFDM m^{-2} (SD = 2.65). *Melanoides* constituted 88% of the total invertebrate biomass during summer 2006.

Specific growth rates for *Melanoides* ranged from 6.9×10^{-4} to 5.7×10^{-2} day^{-1} and declined with body size (Fig. 1). Densities of large snails were low and we were unable to measure growth during the 3-week incubations. We assumed that individuals longer than 13 mm had a specific growth rate of 0 day^{-1}. Water temperatures did not vary enough during the growth incubations to require a temperature component in size-specific growth rate equations.

Secondary production of *Melanoides* biomass in Kelly Warm Springs was 0.43 g AFDM m^{-2} day^{-1} in 2006 (SD = 0.19), with a *P*:*B* of 1.1×10^{-2} day^{-1} (4.1 $year^{-1}$, without accounting for fecundity or potential seasonal changes in growth). The density of fecund individuals was 370 $individuals^{-1}$ m^{-2} in summer 2006, yielding an estimated production of 184 young m^{-2} day^{-1} and a daily production rate of 0.07 g AFDM (of young) m^{-2} day^{-1}. Combining production from the shell growth of the current population with predicted fecundity of individuals 12.0–25.0 mm in length, *Melanoides* produced 0.5 g AFDM m^{-2} day^{-1} and had a *P*:*B* of 4.9 $year^{-1}$ during summer 2006.

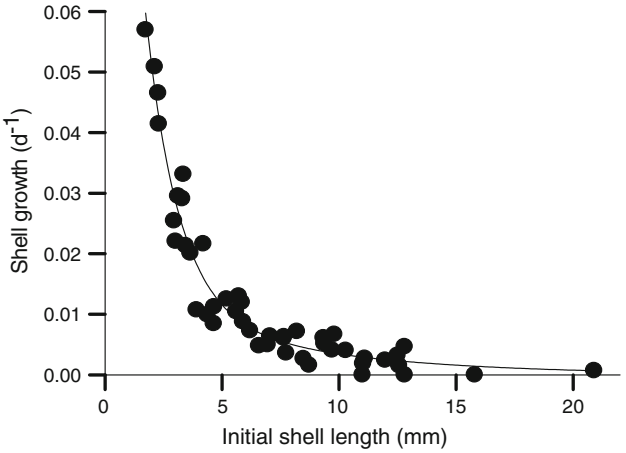

Fig. 1 Snail-specific growth rates of *Melanoides tuberculata* as a function of initial body size (shell length) measured in situ June–September 2006 in Kelly Warm Springs, Grand Teton National Park, Wyoming, USA. Daily shell growth rate is best predicted by $0.0142e^{-0.1454[\text{shell length (mm)}]} + 0.1686e^{-0.7165[\text{shell length (mm)}]}$ ($n = 46$, $r^2 = 0.9507$, $P < 0.0001$)

Shell mass, calculated with direct measurements of *Melanoides* population density and size frequency, was 212 g $CaCO_3$ m^{-2} (90% bootstrap CI = 171–257), or 2.1 mol $CaCO_3$ m^{-2}. Using estimates of shell length distributions and shell growth, *Melanoides* produced 14.1 mmol $CaCO_3$ m^{-2} day^{-1} (SD = 5.0) through biocalcification. Biocalcification by *Melanoides* contributed 12.1 mmol CO_2 m^{-2} day^{-1} to the water column inorganic C pool.

C cycling in Kelly Warm Springs

Temperature, pH, and ANC varied on a diel basis throughout the summer. Temperatures from June to September 2006 ranged from 22.6 to 31.3°C (mean = 27.3°C) along the 504-m reach. ANC and pH averaged 0.0032 mmol m^{-3} and 8.1, respectively, during the same time period (using measurements from every 3 h during 24-h sampling periods).

SF_6 additions yielded a K_{SF_6} value of 0.00155 m^{-1} (95% CI for all three releases = 0.0015–0.0016) and a K_{600} value of 0.00136 m^{-1}. The gas transfer velocity, k_{SF_6}, was 0.00298 m min^{-1} (k_{600} = 15.7 cm h^{-1}). Mean GPP and

Table 1 Measurements of ecosystem respiration (*ER*), gross primary production (*GPP*) and net ecosystem production (*NEP* = GPP − ER) in Kelly Warm Springs during summer 2006

Date measured	ER (mmol $O_2 m^{-2}$ day^{-1})	GPP (mmol O_2 m^{-2} day^{-1})	NEP (mmol O_2 m^{-2} day^{-1})
21–22 July 2006	−544	838	294
27–28 July 2006	−522	375	−147
7–8 August 2006	−591	381	−210
8–9 August 2006	−591	419	−172
10–11 August 2006	−472	375	−97
11–12 August 2006	−472	359	−113
13–14 August 2006	−538	431	−107
Average (without 21–22 July)	−533 (−531)	454 (390)	−79 (−141)
SD (without 21–22 July)	49 (53)	171 (28)	169 (44)

One-station calculations were comparable to metabolism data from two-station calculations, so July 2006 data measured using the one-station, open-channel, dissolved O_2 method are included in the average metabolism rates

Table 2 CO_2 production via calcification by several freshwater and marine organisms

Organism	CO_2 production (mmol CO_2 m^{-2} day^{-1})	Citation
Coral reefs	19.5–268.7	De'ath et al. (2009); Silverman et al. (2009)
Elminius modestus (Australasian barnacle)	10.1–34.8	Golléty et al. (2008)
Dreissena polymorpha (zebra mussels)[a]	0.0–49.3	Chauvaud et al. (2003)[b]
Corbicula fluminea (freshwater Asian clam)[a]	4.9–29.6	Chauvaud et al. (2003)[b]
Melanoides tuberculata (red-rim melania)[a]	8.8–17.8	This study
Potamocorbula amurensis (Asian clam)	0.2–24.1	Chauvaud et al. (2003)
Ophiothrix fragilis (brittle star)	12.1	Migné et al. (1998)
Crepidula fornicata (slipper limpet)	9.9	Martin et al. (2006)
Bryozoans, coralline algae, echinoderms, and mollusks	7.1	Smith (1972)
Bryozoans	1.1	Smith and Nelson (1994)
Pteropod mollusks	0.0091–0.0429	Fabry (1990)
Heteropod mollusks	0.0013–0.0045	Fabry (1990)

Organisms are ranked in descending order of CO_2 production

[a] Freshwater organisms

[b] Calcification values calculated from other sources by Chauvaud et al. (2003)

ER measurements in July and August were 454.0 mmol O_2 m^{-2} day^{-1} and −532.6 mmol O_2 m^{-2} day^{-1} (Table 1), respectively. These fluxes, when converted to CO_2, resulted in −378.4 mmol CO_2 m^{-2} day^{-1} GPP (SD = 142.6) and 532.6 mmol CO_2 m^{-2} day^{-1} ER (SD = 48.9). Mean net ecosystem CO_2 production was 155 mmol CO_2 m^{-2} day^{-1} (SD = 147).

One- and two-station ER measurements differed by an average of 3.8% (n = 3, SD = 2.7), with one-station ER slightly higher than two-station measurements during two out of three measurements periods. The average difference between one- and two-station GPP measurements was 15.8% (n = 5, SD = 2.9). This difference in one- and two-station GPP was the result of consistently higher GPP values from the two-station calculations.

Kelly Warm Springs was always super-saturated with CO_2, and therefore was a net source of CO_2 to the atmosphere. CO_2 partial pressure values ranged from 476 to 5,420 µatm, with a mean of 2,730 µatm over 24-h cycles. CO_2 evasion rates ranged from 0.0097 to 0.32 mmol CO_2 m^{-2} min^{-1}. CO_2 evasion fluxes were higher during late evening and early morning and lower in the afternoon (Fig. 2). Diffusion and re-aeration accounted for a flux of 211.8 mmol CO_2 m^{-2} day^{-1} (SD = 30.6), including losses from high-CO_2 groundwater inputs upstream.

Contributions of *Melanoides* to C cycling

Compared to the daily swings of CO_2 production, consumption and export of CO_2, calcification produced a relatively small amount of CO_2 (Fig. 3). The CO_2 released from biocalcification accounted for 7.3% of net ecosystem CO_2 production. Because the dissolved inorganic C pool

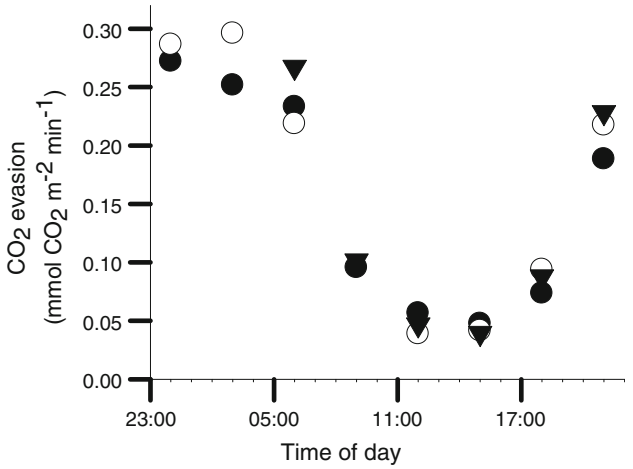

Fig. 2 Net CO_2 evasion from Kelly Warm Springs in 2006 by time of day for 3 days: 27–28 July (*filled circles*), 7–8 August (*open circles*), 10–11 August (*filled triangles*)

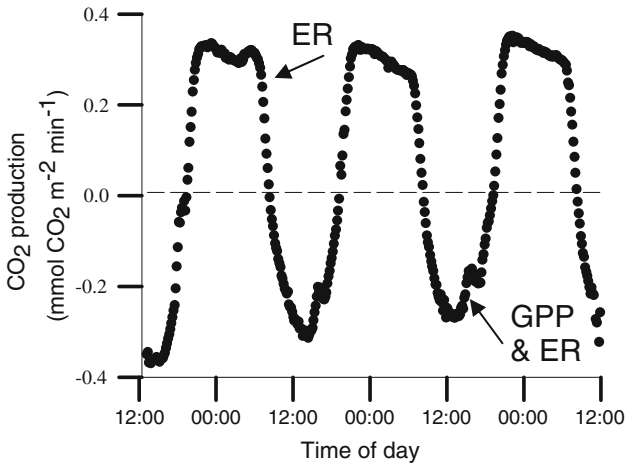

Fig. 3 CO_2 production by *M. tuberculata* calcification (*dashed line*) and diel fluctuations of CO_2 from gross primary productivity (*GPP*) and ecosystem respiration (*ER*) 10–13 August 2006 (metabolism represented by *filled circles*)

was dominated by HCO_3^-, most of the CO_2 produced was transformed to HCO_3^-. Including biocalcification in the inorganic C budget for Kelly Warm Springs increased net ecosystem CO_2 production from 155 to 167 mmol CO_2 m^{-2} day^{-1}.

Discussion

Melanoides production

Warm temperatures and high primary productivity have likely facilitated an extremely high biomass and biomass production by *Melanoides* in Kelly Warm Springs. Biomass production by *Melanoides* (0.43 g AFDM m^{-2} day^{-1}) was similar to rates published for invasive *Potamopyrgus antipodarum* (0.5 g AFDM m^{-2} day^{-1}) in Polecat Creek, Wyoming (Hall et al. 2006) and for *Melanoides* in its native range (0.37 g shell-free dry weight m^{-2} day^{-1}) in Hong Kong (Dudgeon 1986). In comparison, *Melanoides* biomass production was higher than that of the native freshwater snail, *Elimia* spp., in the southeastern United States (0.0068 g AFDM m^{-2} day^{-1}; Huryn et al. 1995). The contribution of fecundity to *Melanoides* secondary production is uncertain, but is likely small in comparison to somatic production, as was found for *Potamopyrgus antipodarum* (Hall et al. 2006). *Melanoides* have lower fecundity rates compared to other successful invasive freshwater snails (Facon et al. 2006). Therefore, it is no surprise that the *Melanoides* *P*:*B* of 4.9 $year^{-1}$ was lower than 12 $year^{-1}$ calculated for the invasive New Zealand mud snail, *Potamopyrgus*, in the greater Yellowstone area (Hall et al. 2006).

Melanoides specific growth rates in Kelly Warm Springs (0.057–0.002 day^{-1}, Fig. 1) were comparable to those reported for *Melanoides* in the literature. Laboratory studies have estimated specific growth rates ranging from 0.016 to 0.004 day^{-1} (Berry and Kadri 1974; Subba Rao and Mitra 1982), with an initial maximum rate of 0.1 day^{-1} (Facon et al. 2005). Size-distribution sampling methods estimated specific growth rates of 0.012–0.003 day^{-1} (Pointier et al. 1993). Our calculations of annual *P*:*B* with and without fecundity (4.1–4.9 $year^{-1}$) were also similar to published *P*:*B* values for *Melanoides* of 4.4 $year^{-1}$ in Lake Kariba, Zimbabwe (Kiibus and Kautsky 1996) and 4.81 $year^{-1}$ in Ping Long, Hong Kong (Dudgeon 1986).

Melanoides densities in growth cages were restricted to avoid food limitation by the end of the 3-week incubations and were also a function of the smaller "depth" in cages versus the stream sediment. As a result, specific growth rates were measured using snail densities at the lower end of the range found in Kelly Warm Springs (the equivalent of 5,000 individuals m^{-2} in cages; ambient density was 29,600 individuals m^{-2} with a SD of 20,500). If our methods did slightly overestimate growth rates because *Melanoides* growth was density dependent (which does not seem likely given the above comparisons of growth and *P*:*B*), our final conclusion that stream CO_2 fluxes dominate calcification CO_2 fluxes is a conservative one.

C cycling in Kelly Warm Springs

Kelly Warm Springs was net heterotrophic during six of the seven diel measurement cycles, despite high rates of GPP. GPP:ER was less than one, suggesting the importance of organic C sources from upstream production, terrestrial inputs and/or in-stream algal production earlier in the summer. Rates of GPP and ER in Kelly Warm Springs

were higher than in most streams (Mulholland et al. 2001; Young et al. 2008) as well as Polecat Creek, another highly productive stream in the greater Yellowstone ecosystem (Hall et al. 2003).

We measured much higher GPP from 21 to 22 July in comparison to the other ecosystem metabolism measurements throughout July and August (Table 1). This high rate of GPP from 21 to 22 July was chiefly responsible for the larger SDs of the mean GPP and net ecosystem production (NEP). Based on the published variability in stream metabolism rates within seasons (Roberts et al. 2007) and the stability of our MiniSonde readings, we do not believe this higher rate of GPP is due to instrument error. Consequently, we included these sampling dates in the metabolism data used to calculate the mean rates of GPP, ER, and NEP for Kelly Warm Springs in 2006.

Photosynthesis and respiration clearly drove 24-h cycles in O_2, CO_2 and, as a result, diel changes in CO_2 evasion (Figs. 2, 3). The 504-m reach was super-saturated with CO_2 with respect to atmospheric concentrations. Although CO_2 concentrations were higher at night, driven by respiration, Kelly Warm Springs was a net source of CO_2 to the atmosphere throughout all of our diel measurements, likely due to CO_2-rich spring water above the reach.

Contributions of *Melanoides* to C cycling

Biocalcification can contribute substantially to ecosystem C cycling (Chauvaud et al. 2003; Wilson et al. 2009). The introduction and establishment of *Melanoides* in Kelly Warm Springs has likely increased biological CO_2 production due to biocalcification and, consequently, has also increased CO_2 evasion from the water into the atmosphere. However, these biocalcification fluxes were small compared to the large daily gross inorganic C fluxes driven by photosynthesis and respiration (Fig. 3).

CO_2 production by *Melanoides* calcification, only a fraction of daily inorganic C cycling in relation to GPP and ER, was 7.3% of the net biological CO_2 production and 5.7% of the daily CO_2 efflux from Kelly Warm Springs (Fig. 4). Diffusion and re-aeration were responsible for the evasion of 39% of total biological CO_2 production (ER + calcification). Holding all other processes equal, the loss of calcifying *Melanoides* could only decrease CO_2 evasion rates from 212 to 207 mmol CO_2 m^{-2} day^{-1}.

Snail production and calcification rates are most likely constrained by primary production and, in general, food availability. It is unlikely that ecosystems will be able to support an excess of invertebrate growth and biocalcification without increased rates of ecosystem metabolism to support this secondary production. Thus, calcifying animals are not likely to constitute a large fraction of gross ecosystem CO_2 fluxes relative to those driven by ecosystem

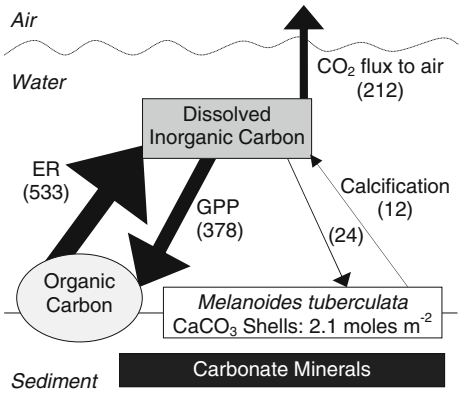

Fig. 4 Carbonate pools and fluxes within and from Kelly Warm Springs. *Arrows* represent fluxes (mmol CO_2 m^{-2} day^{-1}) and *boxes* are standing stocks (mmol m^{-2}; stream depth = 0.124 m). *Arrow widths* show the relative contributions to in-stream CO_2 cycling. *Two arrows* for calcification represent the bicarbonate uptake associated with CO_2 production (2 mol HCO_3^- per mol CO_2), which shifts the carbonate-bicarbonate balance of the inorganic carbon pool. The positive value for ER corresponds to net CO_2 production instead of net production of organic carbon. We did not quantify shell dissolution rates or carbonate minerals in the sediment

metabolism. While gross fluxes are useful in understanding an invasive species' influence on total CO_2 production in an aquatic ecosystem, comparing net fluxes may also yield important conclusions about the impact of invasive species on the relative balance of ecosystem C cycling. For example, in an ecosystem with large, but relatively equal GPP and ER rates, biocalcification by an invasive species could potentially alter the CO_2 balance of that ecosystem.

Melanoides have thicker shells and are larger than the other mollusks present in Kelly Warm Springs, so the shell mass of *Melanoides* could also alter inorganic C cycling. $CaCO_3$ production by *Melanoides* may approach annual rates of more than 500 g $CaCO_3$ m^{-2} $year^{-1}$. *Melanoides* shells will take several years to dissolve after death, especially with high Ca concentrations (Ca^{2+}) and pH in Kelly Warm Springs, which impede $CaCO_3$ dissolution (Strayer and Malcom 2007). We do not have sufficient data to quantify how dissolving shells contribute to the net impact of *Melanoides* on stream CO_2 fluxes. But if the gross flux (calcification only) is minimal when compared to stream CO_2 fluxes, we expect net fluxes (calcification and shell dissolving rates) to be an even smaller proportion of whole-ecosystem CO_2 cycling.

Our study focused on the direct effects that *Melanoides* have on inorganic C cycling, but *Melanoides* likely have indirect effects on ecosystem C cycling that may be far more substantial than those calculated for increases in CO_2 production by biocalcification. Published indirect effects on aquatic C cycling by changing densities of animals include increased rates of ER and GPP after the exclusion of a sediment-feeding fish species (Taylor et al. 2006) and

altered ecosystem CO_2 fluxes into the atmosphere after changing densities of top predators (Schindler et al. 1997). Respiration by exotic zebra mussels (*Dreissena polymorpha*) significantly decreased O_2 concentrations in the Hudson River (Caraco et al. 2000). Hudson River phytoplankton biomass also declined as a result of grazing pressure by zebra mussels (Caraco et al. 1997). Similarly, *Melanoides* could indirectly alter rates of GPP and ER through heavy grazing on algae in ecosystems where they have reached high biomass densities.

This study evaluated the potential role of invasive species as an additional source of CO_2 to stream inorganic C budgets. *Melanoides* dominated total invertebrate biomass, and calcification by *Melanoides* increased total CO_2 production and evasion. The calcification-driven CO_2 fluxes were large and within the range of those reported for other calcifying organisms in the literature. Despite this large biocalcification flux, the increase in net ecosystem CO_2 production was small when compared to ecosystem-level C fluxes from GPP and ER. Species-level influences on C cycling should always be compared to whole-ecosystem processes and fluxes in order to accurately understand how animals can alter biological and geochemical processes in aquatic ecosystems.

Acknowledgments We thank E. Pendall, A. Krist, D. Strayer, E. Hansen, A. Ulseth, L. Kunza and two anonymous reviewers for helpful comments on earlier drafts of our manuscript. S. O'Ney and H. Harlow provided logistical support. R. Crosby, J. Theurer, N. Swoboda-Colberg, and T. Lehnertz assisted with field and lab work. Discussions with J. Meyer also contributed to this research. This project was funded by a University of Wyoming–National Park Service research grant. Research was also supported by a Plummer Scholarship (School of Environment and Natural Resources, University of Wyoming), a Dennis Jesperson Memorial Scholarship (Wyoming Wildlife Fund), and a Colorado Lake and Reservoir Management Association Scholarship. This manuscript is a contribution to the University of Wyoming–National Park Service Research Station.

References

Benke AC (1984) Secondary production of aquatic insects. In: Resh VH, Rosenberg DM (eds) Ecology of aquatic insects. Praeger, New York, pp 289–322

Benke AC, Huryn AD, Smock LA, Wallace JB (1999) Length-mass relationships for freshwater macroinvertebrates in North America with particular reference to the southeastern United States. J North Am Benthol Soc 18:308–343

Berry AJ, Kadri ABH (1974) Reproduction in the Malayan freshwater cerithiacean gastropod *Melanoides tuberculata*. J Zool 172: 369–381

Cai W-J, Wang Y (1998) The chemistry, fluxes, and source of carbon dioxide in the estuarine waters of the Satilla and Altamaha Rivers, Georgia. Limnol Oceanogr 43:657–668

Caraco NF, Cole JJ, Raymond PA, Strayer DL, Pace ML, Findlay SEG, Fischer DT (1997) Zebra mussel invasion in a large, turbid river: phytoplankton response to increased grazing. Ecology 78:588–602

Caraco NF, Cole JJ, Findlay SEG, Fischer DT, Lampman GG, Pace ML, Strayer DL (2000) Dissolved oxygen declines in the Hudson River associated with the invasion of the zebra mussel (*Dreissena polymorpha*). Environ Sci Technol 34:1204–1210

Chauvaud L, Thompson JK, Cloern JE, Thouzeau G (2003) Clams as CO_2 generators: the *Potamocorbula amurensis* example in San Francisco Bay. Limnol Oceanogr 48:2086–2092

Cole JJ, Caraco NF (1998) Atmospheric exchange of carbon dioxide in a low wind oligotrophic lake measured by the addition of SF_6. Limnol Oceanogr 43:647–656

Cole JJ, Caraco NF, Kling GW, Kratz TK (1994) Carbon dioxide supersaturation in the surface waters of lakes. Science 265:1568–1570

Cole JJ, Pace ML, Carpenter SR, Kitchell JF (2000) Persistence of net heterotrophy in lakes during nutrient additions and food web manipulations. Limnol Oceanogr 45:1718–1730

Cole JJ, Prairie YT, Caraco NF, McDowell WH, Tranvik LJ, Striegl RG, Duarte CM, Kortelainen P, Downing JA, Middleburg JJ, Melack J (2007) Plumbing the global carbon cycle: integrating inland waters into the terrestrial carbon budget. Ecosystems 10:171–184

De'ath G, Lough JM, Fabricius KE (2009) Declining coral calcification on the Great Barrier Reef. Science 323:116–119

Duarte CM, Prairie YT (2005) Prevalence of heterotrophy and atmospheric CO_2 emissions from aquatic ecosystems. Ecosystems 8:862–870

Dudgeon D (1986) The life cycle, population dynamics and productivity of *Melanoides tuberculata* (Müller, 1774) (Gastropoda: Prosobranchia: Thiaridae) in Hong Kong. J Zool 208:37–53

Duggan IC (2002) First record of a wild population of the tropical snail *Melanoides tuberculata* in New Zealand natural waters. NZ J Mar Freshwater Res 36:825–829

Fabry VF (1990) Shell growth rates of pteropod and heteropod molluscs and aragonite production in the open ocean: implications for the marine carbonate system. J Mar Res 48:209–222

Facon B, Pointer J-P, Glaubrecht M, Poix C, Jarne P, David P (2003) A molecular phylogeography approach to biological invasions of the New World by parthenogenetic Thiarid snails. Mol Ecol 12:3027–3039

Facon B, Jarne P, Pointier JP, David P (2005) Hybridization and invasiveness in the freshwater snail *Melanoides tuberculata*: hybrid vigor is more important than increase in genetic variance. J Evol Biol 18:524–535

Facon B, Genton BJ, Shykoff J, Jarne P, Estoup A, David P (2006) A general eco-evolutionary framework for understanding bioinvasions. Trends Ecol Evol 21:130–135

Frankignoulle M, Canon C, Gattuso J-P (1994) Marine calcification as a source of carbon dioxide: positive feedback of increasing atmospheric CO_2. Limnol Oceanogr 39:458–462

Golléty C, Gentil F, Davoult D (2008) Secondary production, calcification and CO_2 fluxes in the cirripedes *Chthamalus montagui* and *Elminius modestus*. Oecologia 155:133–142

Hall RO, Tank JL (2005) Correcting whole-stream estimates of metabolism for groundwater input. Limnol Oceanogr Methods 3:222–229

Hall RO, Tank JL, Dybdahl MF (2003) Exotic snails dominate nitrogen and carbon cycling in a highly productive stream. Front Ecol Environ 1:407–411

Hall RO, Dybdahl MF, VanderLoop MC (2006) Extremely high secondary production of introduced snails in rivers. Ecol Appl 16:1121–1131

Hall RO, Thomas S, Gaiser EE (2007) Measuring primary production and respiration in freshwater ecosystems. In: Fahey TJ, Knapp

AK (eds) Principles and standards for measuring primary production. Oxford University Press, Oxford, pp 175–203
Huryn AD, Benke AC, Ward GM (1995) Direct and indirect effects of geology on the distribution, biomass, and production of the freshwater snail *Elimia*. J North Am Benthol Soc 14:519–534
Jones JB, Mulholland PJ (1998) Influence of drainage basin topography and elevation on carbon dioxide and methane supersaturation of stream water. Biogeochemistry 40:57–72
Kiibus M, Kautsky N (1996) Respiration, nutrient excretion and filtration rate of tropical freshwater mussels and their contribution to production and energy flow in Lake Kariba, Zimbabwe. Hydrobiologia 331:25–32
Langmuir D (1997) Aqueous environmental chemistry. Prentice Hall, Upper Saddle River
Martin S, Thouzeau G, Chauvaud L, Jean F, Guérin L, Clavier J (2006) Respiration, calcification, and excretion of the invasive slipper limpet, *Crepidula fornicata* L.: implications for carbon, carbonate, and nitrogen fluxes in affected areas. Limnol Oceanogr 51:1996–2007
Migné A, Davoult D, Gattuso J-P (1998) Calcium carbonate production of a dense population of the brittle star *Ophiothrix fragilis* (Echinodermata: Ophiuroidea): role in the carbon cycle of a temperate coastal ecosystem. Mar Ecol Prog Ser 173: 305–308
Millero FJ (1979) The thermodynamics of the carbonate system in seawater. Geochim Cosmochim Acta 43:1651–1661
Mulholland PJ, Fellows CS, Tank JL, Grimm NB, Webster JR, Hamilton SK, Martí E, Ashkenas L, Bowden WB, Dodds WK, McDowell WH, Paul MJ, Peterson BJ (2001) Inter-biome comparison of factors controlling stream metabolism. Freshwater Biol 46:1503–1517
Odum HT (1956) Primary production in flowing waters. Limnol Oceanogr 1:102–117
Pointier JP, Delay B, Toffart JL, Lefevre M, Romero-Alvarez R (1992) Life history traits of three morphs of *Melanoides tuberculata* (Gastropoda: Thiaridae), an invading snail in the French West Indies. J Mollusc Stud 58:415–423
Pointier JP, Théron A, Borel G (1993) Ecology of the introduced snail *Melanoides tuberculata* (Gastropoda: Thiaridae) in relation to *Biomphalaria glabrata* in the marshy forest zone of Guadeloupe, French West Indies. J Mollusc Stud 59:421–428
R Development Core Team (2009) R: a language and environment for statistical computing. Vienna
Rader RB, Belk MC, Keleher MJ (2003) The introduction of an invasive snail (*Melanoides tuberculata*) to spring ecosystems of the Bonneville Basin, Utah. J Freshwater Ecol 18:647–657
Raine RCT (1983) The effect of nitrogen supply on the photosynthetic quotient of natural phytoplankton assemblages. Bot Mar 26:417–423
Richey JE, Melack JM, Aufdenkampe AK, Ballester MV, Hess LL (2002) Outgassing from Amazonian rivers and wetlands as a large tropical source of atmospheric CO_2. Nature 416:617–620
Roberts BJ, Mulholland PJ, Hill WR (2007) Multiple scales of temporal variability in ecosystem metabolism rates: results from 2 years of continuous monitoring in a forested headwater stream. Ecosystems 10:588–606
Robinson DG (1999) Alien invasions: the effects of the global economy on non-marine gastropod introductions into the United States. Malacologia 41:413–438
SAS Institute (2002–2003) SAS/STAT User's Guide, Release 9.1.3. SAS Institute, Cary
Schindler DE, Carpenter SR, Cole JJ, Kitchell JF, Pace ML (1997) Influence of food web structure on carbon exchange between lakes and the atmosphere. Science 277:248–251
Silverman J, Lazar B, Cao L, Caldeira K, Erez J (2009) Coral reefs may start dissolving when atmospheric CO_2 doubles. Geophys Res Lett 36:L05606. doi:10.1029/2008GL036282
Smith SV (1972) Production of calcium carbonate on the mainland shelf of southern California. Limnol Oceanogr 17:28–41
Smith AM, Nelson CS (1994) Calcification rates of rapidly colonizing bryozoans in Hauraki Gulf, northern New Zealand. NZ J Mar Freshwater Res 28:227–234
Strayer DL, Malcom HM (2007) Shell decay rates of native and alien freshwater bivalves and implications for habitat engineering. Freshwater Biol 52:1611–1617
Strayer DL, Caraco NF, Cole JJ, Findlay S, Pace ML (1999) Transformation of freshwater ecosystems by bivalves: a case study of zebra mussels in the Hudson River. Bioscience 49:19–27
Subba Rao NV, Mitra SC (1982) Bioecology of two melaniid snails (Mollusca: Gastropoda) in ponds near Calcutta. J Zool Soc (India) 1&2:21–32
Taylor BW, Flecker AS, Hall RO (2006) Loss of a harvested fish species disrupts carbon flow in a diverse tropical river. Science 313:833–836
United States Geological Survey (2005) Nonindigenous aquatic species database, Gainesville. http://nas.er.usgs.gov. Accessed Mar 2007
Wanninkhof R (1992) Relationship between wind speed and gas exchange over the ocean. J Geophys Res 97:7373–7382
Wanninkhof R, Mulholland PJ, Elwood JW (1990) Gas exchange rates for a first order stream determined with deliberate and natural tracers. Water Resour Res 26:1621–1630
Ware JR, Smith SV, Reaka-Kudla ML (1991) Coral reefs: sources or sinks of atmospheric CO_2? Coral Reefs 11:127–130
Wetzel RG (2001) Limnology, 3rd edn. Academic Press, San Diego
Wetzel RG, Likens GE (2000) Limnological analyses, 3rd edn. Springer, New York
Williams PB, del Giorgio PA (2005) Respiration in aquatic ecosystems: history and background. In: del Giorgio PA, Williams PB (eds) Respiration in aquatic ecosystems. Oxford University Press, Oxford, pp 1–17
Wilson RW, Millero FJ, Taylor JR, Walsh PJ, Christiansen V, Jennings S, Grosell M (2009) Contribution of fish to the marine inorganic carbon cycle. Science 323:344–359
Young RG, Matthaei CD, Townsend CR (2008) Organic matter breakdown and ecosystem metabolism: functional indicators for assessing river ecosystem health. J North Am Benthol Soc 27:605–625